Atomic force microscopy

Tone Reversal of an AFM Lateral Force Image Due to Hybridization of Oligonucleotides Immobilized on Polymers

Dan V. Nicolau, Duy K. Pham, Elena P. Ivanova, Jonathan P. Wright, Ralf Lenigk, Thomas Smekal, and Piotr Grodzinski*

The immobilization and molecular conformation of oligonucleotides on surfaces is critical to DNA-based microdevices, such as biosensors,[1] micro- and nanoarrays,[2,3] and lab-on-a-chip devices.[4] Traditionally, these devices use glass or silicon as the base material, which have well characterized surface chemistry. However, the increasing demand for DNA-based microdevices requires low-cost, easily processable materials that could be suitable for disposable devices. The use of polymers, which are the logical choice from the manufacturing point of view, is however challenged by two sets of fundamental problems. Firstly, as polymer bulk properties (relevant to manufacturing) need to be decoupled from surface properties (relevant to biomolecule immobilization), additional surface functionalization is usually needed for covalent binding of oligonucleotides.[5–11] Plasma processing, which changes only the very top surface of the polymer, has been widely used for polymer processing[12] but not for DNA-based microdevices. The second, less apparent, challenge is the complexity and dynamic character of the polymer surface compared with, for example, glass. Consequently, the key performance criteria of oligonucleotide immobilization on surfaces, i.e., a high density of bound target molecule and favorable molecular conformation, have to be reconsidered with respect to the interaction of oligonucleotide chains, themselves of a quasi-polymeric nature, with the polymer surface. Atomic force microscopy (AFM) is commonly used for the mapping of nanotopography, but also of spatial distribution of oligonucleotides' chemistry[13] and hydrophobicity,[14] and the local mechanical properties of polymers.[15] AFM has also been used to visualize individual DNA molecules[16–19] and, recently, to fabricate DNA nanoarrays.[3]

This communication reports on the use of two very different polymers, both good candidates for the fabrication of bio-microdevices, that is, polycarbonate (PC)[4] and cyclo-olefin copolymer (COC),[20] for probing the interaction between oligonucleotides during immobilization and hybridization. This communication also reports on the use of AFM, and in particular the lateral force (LF), as a means to detect the immobilization and hybridization of oligonucleotides on polymers.

Although the model polymers have similar thermo-mechanical properties (glass transition temperature, T_g, of 136 °C and 145 °C, for COC and PC, respectively), their different chemistry translates into very different processes induced by plasma treatment, which are confined to the top 200 nm.[12] Firstly, the [total O]/[total C] atomic ratio increases from 15.5 % to 21.5 % for COC samples, and decreases from 45.2 % to 26.7 % for PC samples. Secondly, the [oxygen-bound carbon (C_xO_y)]/[total C] ratio increases for COC from 15.5 % to 21.5 % over the full duration of plasma processing (up to 5 min), but decreases dramatically for PC during the first 20 s of plasma treatment (from 45 % to 29 %) and further decreases to 26 % at the end of the process (Figure 1). These data suggest that the opening of the norbornene ring of COC, supported by the decrease of the [CH_x]/[total C] atomic ratio, produces a linear aliphatic polymer, which, in turn, result in a significant decrease of the local stiffness of the polymer. On the other hand, the already more rigid PC surface (due to bulkier aromatic groups) is further stiffened by plasma processing due to localized crosslinking.[21] Hence, the relatively softer COC top surface coupled with the long incubation in *N*-hydroxysuccinimide (NHS) solution (6 h) also leads to more-advanced functionalization than for the PC surface due to more-ad-

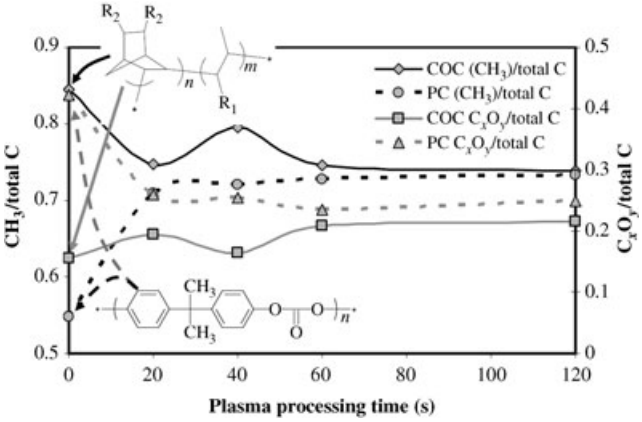

Figure 1. Evolution of the atomic ratios for COC (full lines) and PC (dotted lines) of [aliphatic C]/[total C] (black lines) and [O-bound C]/[total C] (grey lines). The starting structures of the polymers before plasma processing are presented for COC (top) and PC (bottom). R_1 and R_2 represent aliphatic side-chains.

[*] Prof. D. V. Nicolau, Dr. D. K. Pham, Dr. E. P. Ivanova, Dr. J. P. Wright
Faculty of Engineering & Industrial Sciences
Swinburne University of Technology Hawthorn
Victoria, 3122 (Australia)
Fax: +61-392-145-050
E-mail: dnicolau@swin.edu.au

Dr. R. Lenigk,[+] Dr. T. Smekal,[+] Dr. P. Grodzinski[++]
Microfluidics Laboratory, Motorola Physical Sciences Laboratories
Tempe, Arizona (USA)

[+] Current address:
Applied NanoBioscience Center, Arizona State University, Tempe, Arizona (USA)

[++] Current address:
Los Alamos National Laboratory, Bioscience Division, MS J586, Los Alamos, New Mexico (USA)

Supporting information for this article is available on the WWW under http://www.small-journal.com or from the author.

  DOI: 10.1002/smll.200400125

vanced polymer swelling and unfolding of the polymeric chains. The LF increase for COC bare, plasma-treated, and NHS-functionalized surfaces, which could be a result of higher hydrophilicity[14] due to C_xO_y species and/or lower local stiffness,[15] compared with the LF decrease for the respective PC samples, further supports the above model.

The similarity of noncontact and contact mode AFM images of the covalently bound oligonucleotides aggregates on both polymer surfaces suggests that the oligonucleotides are strongly bound to the polymer surface. The coverage of the surface with oligonucleotide aggregates is 41.25% and 16.94% for COC and PC, respectively. A remarkable aspect of the ssDNA immobilization is the considerable height of the aggregates, i.e., 61.4 nm and 28.5 nm for COC and PC samples, respectively. Similar heights (i.e., 20–50 nm) for similar oligonucleotide lengths (i.e., 25–30 bases) have been also reported for oligonucleotide films immobilized on plasma-polymerized surfaces.[22] As proposed above, the swelling and chain unfolding during the long ssDNA immobilization (6 h) coupled with a higher concentration of NHS groups grafted on the flexible polymeric chains results in a higher concentration of ssDNA on COC than PC surfaces.

Interestingly, the ssDNA aggregates are apparently hydrophobic, as suggested by the lower LF acquired on oligonucleotide aggregates on both polymers (darker spots in Figure 2 top two inset images). Figure 3 (bivariate histogram analysis, top two clusters) shows a clear decrease of the LF with the increase in topography (negative slope of LF-topography "cloud"). It has been hypothesized[23] that the electrostatic interactions on hydrophilic surfaces orient the oligonucleotide phosphate groups towards the surface, and the molecule would then present the hydrophobic bases pointing upwards. Conversely, on hydrophobic surfaces, the bases orient towards the surface, presenting the hydrophilic phosphate groups upwards. The apparent relative hydrophilicity of the oligonucleotide aggregates suggests a similar mechanism of molecular arrangement. The flexible chains on top of the polymer, which are grafted to the oligonucleotides, allow the orientation of the free bases outwards, creating a molecularly hydrophobic surface.

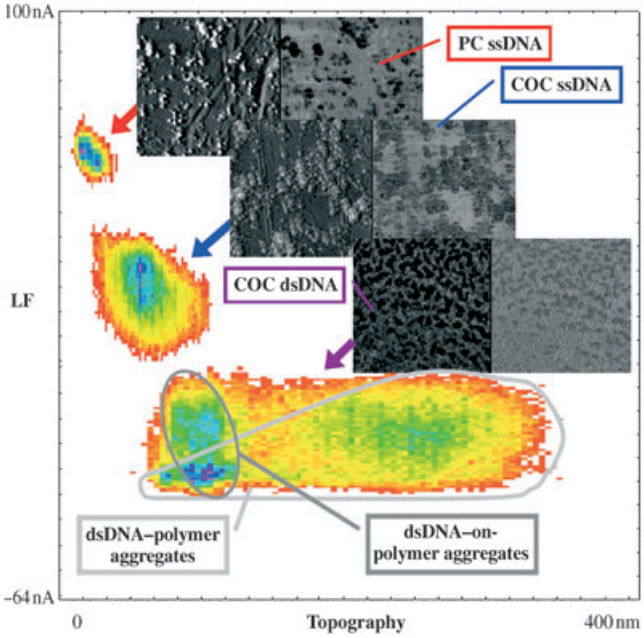

Figure 3. Bivariate histogram analysis for PC ssDNA–polymer aggregates (top left cluster), COC ssDNA–polymer aggregates (middle left cluster), and COC hybridized surfaces (bottom, unhybridized ssDNA aggregates on the subcluster on the left and dsDNA aggregates on the subcluster on the right). The clusters represent the frequency of given LF-topography pairs; the distributions of frequencies are represented by a rainbow-colored code, that is, the highest frequency is shown in purple, and the lowest in red; areas with no data are shown in white. The insets represent AFM images for topography (left) and LF (right). The tone reversal in LF images is evident when comparing the far-left images of the middle and bottom insets, respectively.

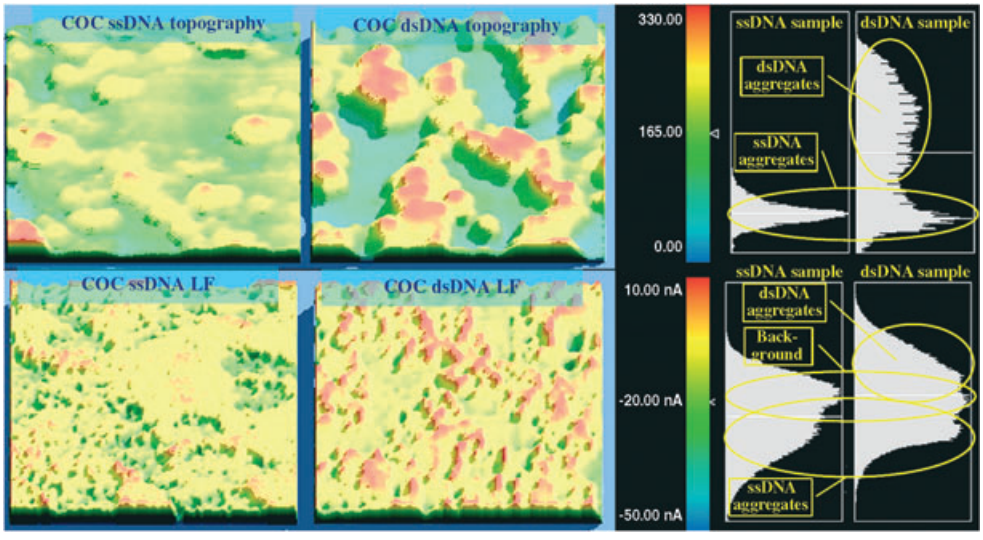

Figure 2. Evolution of the nano-topography (top) and friction caused by lateral force (bottom) for COC surfaces with covalently bound (ssDNA) and hybridized (dsDNA) oligonucleotides (left and right, respectively). The histograms on the far right represent the distribution of topographies (nm) and lateral forces (relative nA) for ssDNA and dsDNA samples.

The hybridization occurred within detectable limits only on ssDNA–COC surfaces (no Cy5 fluorescence was detected on PC samples). Moreover, while the average aggregate height tripled on COC samples (from 61.4 nm to 191 nm), the PC samples underwent a further leveling of the surface (decrease of average height from 28.5 nm to 11.25 nm). This opposite behavior on PC samples can be explained by the fact that the crosslinked

chains drastically limit the access of complementary oligonucleotides and that the long incubation in the hybridization solution causes only further relaxation of the ssDNA–polymer chains. On COC the hybridization results in a modest increase of the dsDNA aggregates in lateral dimensions (i.e., from 41.25% to 59.9% area coverage) compared with the increase of aggregate heights. The difference in growth of the dsDNA aggregates in vertical and lateral dimensions can be explained by specific hybridization, but also by the same mechanism of swelling and unfolding of ssDNA-polymer chains proposed for NHS functionalization and oligonucleotide immobilization (Figure 4).

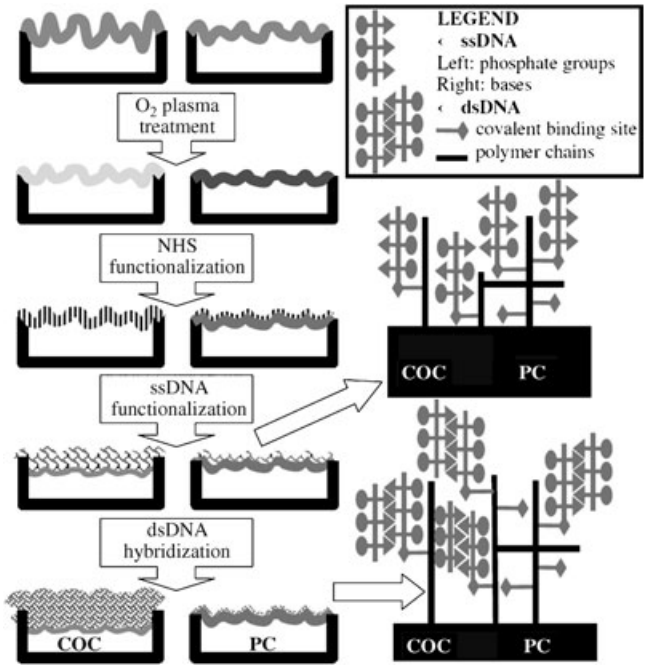

Figure 4. Proposed model of the polymer surface processes prior to and after oligonucleotide immobilization and hybridization. The schemes on the left and right represent COC- and PC-related processes, respectively.

Again, the most interesting results regarding hybridization are revealed by LF analysis, which demonstrates that the surface of the dsDNA aggregates is hydrophilic. This hydrophobicity reversal from ssDNA to dsDNA aggregates (Figure 2, for COC samples only, and insets in Figure 3) can be explained by the flexibility of the ssDNA–COC chain aggregates, which allows an easy access of complementary oligonucleotide molecules and, subsequently, a more-advanced hybridization. This hybridization blocks the previously free bases, which were responsible for the relative hydrophobicity of the ssDNA-polymeric chain aggregates, and now exposes preferentially the hydrophilic phosphate groups. While for ssDNA–polymer aggregates on PC and COC surfaces there is a clear tendency of a decrease of the LF with increased height of the aggregates (i.e., the negative slope of the top two clusters in Figure 3), the dsDNA–polymer aggregates (on COC only) present the opposite behavior (larger subcluster on the bottom cluster in Figure 3) and a tone reversal of the respective LF images. Moreover, the incomplete process of hybridization results in two aggregate populations (Figure 3, bottom cluster).

This contribution demonstrates both the opportunities and the challenges of using polymers for oligonucleotide immobilization and hybridization. The study suggests that softer polymers, especially at the very top layers, should allow more flexibility of the ssDNA–polymer chains and therefore a better efficiency of hybridization. The study also demonstrates the use of AFM lateral force analysis as a global probe of the molecular orientation of the DNA strands, with ssDNA aggregates being relatively hydrophobic and dsDNA aggregates being relatively hydrophilic. The method has the potential to be used to detect hybridization, especially for DNA nanoarrays.

Experimental Section

Polymer surfaces. Poly(ethylene-co-norbornene), known as cyclo-olefin copolymer (COC), and poly(bisphenol A carbonate), known as polycarbonate (PC), were purchased from Ticona, (NJ, USA) and Piper Plastics, (AZ, USA), respectively. The polymer surfaces were treated with oxygen plasma at 100 W for periods ranging from 20 s to 5 min at atmospheric pressure and then functionalized with *N*-hydroxysuccinimide (NHS) as described elsewhere.[4]

Oligonucleotide immobilization. A 26-base-pair oligonucleotide primer FAM-GTG-GAT CAC-CTG-AGG-TCA-GGA-GTT-TC (corresponding to the alu gene), which was amino-modified at the 3′-terminus, was used for covalent binding on polymers. A 20 nmol mL^{-1} solution of oligonucleotide in 150 mM sodium phosphate at pH 8.5 was placed on the NHS-functionalized surface for 6 h at 22 °C and constant humidity, and then washed thoroughly.

Hybridization of oligonucleotides. The prehybridization solution, containing 0.15 M NaCl, 0.015 M sodium citrate, 5× Denhardt's solution, at pH 7.0, was applied to the sample for 10 min. A 40 nmol mL^{-1} solution of the complementary oligonucleotide, Cy5-CA-CCT-GGT-GGA-CTC-CAG-TCC-TCA-AAGG, dissolved in 5× SSC buffer, was applied to the surfaces with immobilized primers. After incubation at 42 °C for 4 h, the slides were washed thoroughly three times with 6× SSC buffer and 0.1% SDS.

Surface characterization. A TopoMetrix Explorer (Thermo-Microscopes) was used for AFM analysis, which was carried out at 23 °C and 45% relative humidity, in both noncontact and contact modes, with a field of view ranging from 2×2 to 100×100 mm^2. The experiments were run in a clean room with controlled temperature and humidity to suppress the sensitivity of AFM experiments to environmental conditions. The image subtraction, RMS, and surface-roughness calculations were performed with the Explorer software. The XPS elemental analyses were carried out on a Kratos Ultra Imaging X-Ray Photoelectron Spectrometer. The analysis areas were approx. 300×700 mm^2. Wide-scan and region-scan spectra were acquired at 160 eV and 20 eV pass-energies, respectively.

Assessment of oligonucleotide immobilization and hybridization. The oligonucleotide immobilization and hybridization was

analyzed qualitatively by fluorescence imaging, then by a quantitative estimation of the additional oligonucleotide volume on the surfaces by AFM topographic measurements of the features rising above the baseline and which have different chemistry (as inferred from their distinct LF) to the background material. Unfortunately, both polymers, but especially PC, present background fluorescence, which renders a quantitative comparison between fluorescence and AFM-based analysis inadequate. Therefore, fluorescence detection could only be used for qualitative assessment. Image analysis was performed with the GelPro Analyzer software (Media Cybernetics, Inc.) and statistical analysis with Statistica 6. (StatSoft, Inc.). In order to reveal the correlation between the oligonucleotide single/double-stranded state and LF, the values of the height and relative friction from each pixel of the corresponding topographic and LF images for ssDNA and dsDNA aggregates were statistically compared and plotted in bivariate histograms.

Acknowledgments

The research was supported by grants from Motorola and the Defense Advanced Research Projects Agency. The authors thank Drs. Paul Pigram and Narelle Brack for XPS analysis.

Keywords:
AFM · DNA immobilization · DNA recognition · lateral force analysis · surfaces

[1] H. Du, M. D. Disney, B. L. Miller, T. D. Krauss, *J. Am. Chem. Soc.* **2003**, *125*, 4012.
[2] S. P. A. Fodor, J. L. Read, M. C. Pirrung, L. Stryer, A. T. Lu, D. Solas, *Science* **1991**, *251*, 767.
[3] L. M. Demers, D. S. Ginger, S.-J. Park, Z. Li, S.-W. Chung, C. A. Mirkin, *Science* **2002**, *298*, 1836.
[4] R. Lenigk, R. H. Liu, M. Athavale, Z. J. Chen, D. Ganser, J. N. Yang, C. Rauch, Y. J. Liu, B. Chan, H. N. Yu, M. Ray, R. Marrero, P. Grodzinski, *Anal. Biochem.* **2002**, *311*, 40.
[5] T. Koch, N. Jacobsen, J. Fensholdt, U. Boas, M. Fenger, M. H. Jakobsen, *Bioconjugate Chem.* **2000**, *11*, 474.
[6] F. Fixe, M. Dufva, P. Telleman, C. B. V. Christensen, *Lab Chip* **2004**, *4*, 191.
[7] H. Kohsaka, A. Taniguchi, D. D. Richman, D. A. Carson, *Nucleic Acids Res.* **1993**, *21*, 3469.
[8] J. A. Running, M. S. Urdea, *BioTechniques* **1990**, *8*, 276.
[9] J. E. Beecher, G. H. McGall, M. Goldberg, *Polym. Mater. Sci. Eng.* **1997**, *76*, 394.
[10] R. S. Matson, J. Rampal, S. L. Pentoney, P. D. Anderson, P. Coassin, *Anal. Biochem.* **1995**, *224*, 110.
[11] A. Sreekumar, M. K. Nyati, S. Varambally, T. R. Barrette, D. Ghosh, T. S. Lawrence, A. M. Chinnaiyan, *Cancer Res.* **2001**, *61*, 7585; J. Weiler, J. D. Hoheisel, *Anal. Biochem.* **1996**, *243*, 218.
[12] S. H. Wheale, J. P. S. Badyal, in *IUPAC Series Chemistry for the 21 st Century*, Interfacial Science Blackwell Science, Oxford, **1997**, chap. 10.
[13] J. C. O'Brien, J. T. Stickney, M. D. Porter, *J. Am. Chem. Soc.* **2000**, *122*, 5004.
[14] N. J. Brewer, B. D. Beake, J. G. Leggett, *Langmuir* **2001**, *17*, 1970.
[15] S. N. Magonov, D. H. Reneker, *Annu. Rev. Mater. Sci.* **1997**, *27*, 175.
[16] E. Casero, M. Darder, D. J. Diaz, F. Pariente, J. A. Martin-Gago, H. Abruna, E. Lorenzo, *Langmuir* **2003**, *19*, 6230.
[17] Y. Fang, J. H. Hoh, *Nucleic Acids Res.* **1998**, *26*, 588.
[18] L. S. Shlyakhtenko, A. A. Gall, J. J. Weimer, D. D. Hawn, Y. L. Lyubchenko, *Biophys. J.* **1999**, *77*, 568.
[19] N. H. Thomson, B. L. Smith, N. Almqvist, L. Schmitt, M. Kashlev, E. T. Kool, P. K. Hansma, *Biophys. J.* **1999**, *76*, 1024.
[20] Y. Yang, J. Kameoka, T. Wachs, J. D. Henion, H. G. Craighead, *Anal. Chem.* **2004**, *76*, 2568.
[21] A. Höfrichter, P. Bulkin, B. J. Drevillon, *J. Vac. Sci. Technol. A* **2002**, *20*, 245.
[22] Z. Zhang, Q. Chen, W. Knoll, R. Foerch, R. Holcomb, D. Roitman, *Macromolecules* **2003**, *36*, 7689.
[23] V. Chan, S. E. McKenzie, S. Surrey, P. Fortina, D. J. Graves, *J. Colloid Interface Sci.* **1998**, *203*, 197.

Received: November 10, 2004

